Electronic Supplementary Information

Synthesis of mesoporous lanthanum hydroxide with enhanced adsorption performance for phosphate removal

Kyungmin Kim,† Dujin Kim,† Taeyeon Kim, Bong-Geun Kim, Donghyun Ko, Junsoo Lee, Yujin Han, Ji Chul Jung, and Hyon Bin Na*

Department of Chemical Engineering, Myongji University, Yongin, Gyeonggi-do 17058, Republic of Korea

*Corresponding author. E-mail: hyonbin@mju.ac.kr (H. B. Na)

†These authors (K. Kim, D. Kim) have contributed equally to this work.

Table S1. Structure characteristics of KIT-6.

Sample	BET surface area (m^2/g)	Pore diameter[a] (nm)	Wall thickness[b] (nm)	Total pore volume (cm^3/g)
KIT-6-35C	645	4.4	4.4	0.76
KIT-6-100C	810	5.9	4.7	1.30

[a] The pore diameter was calculated from the desorption isotherm by the Barrett-Joiner-Halenda (BJH) method. [b] The wall thickness was estimated by TEM analysis.

Table S2. Langmuir and Freundlich isotherm parameters of phosphate adsorption by the synthesized mesoporous lanthanum hydroxides (MLHOs).

Sample	Langmuir			Freundlich		
	q_m (mg/g)	K_L (L/mg)	R^2	n	K_F (mg/g)	R^2
MLHO-100C-2	109.41	63.47	0.9999	7.51	92.70	0.4956
MLHO-100C-3	93.90	11.13	0.9991	8.77	70.57	0.2924
MLHO-100C-4	90.91	3.81	0.9958	6.62	63.18	0.4723
MLHO-35C-2	98.62	18.32	0.9995	5.50	75.79	0.8391
MLHO-35C-3	80.32	27.43	0.9996	7.96	65.21	0.4413
MLHO-35C-4	76.10	9.32	0.9989	5.78	56.11	0.6955

Table S3. Comparison of phosphate adsorption capacity for various La-based adsorbents.

Adsorbent	Adsorption temperature (°C)	q_m (mg/g)	C_o range (mg P/L)	Dosage (g/L)	Surface area (m^2/g)	Ref.
MLHO-100C-2	28	109.41	2-50	0.25	349	This study
Amorphous $La(OH)_3$	25±1	107.53	5-500	2.5	153.3	1
La_2O_3	25±1	46.95	5-500	2.5	12.0	2
$La(OH)_3$-modified exfoliated vermiculites (La_5/EV)	25	79.6	1-100	1.0	39.1	3
	30	75.8				
La-doped ordered mesoporous hollow silica spheres (HMS-1/5)	25	47.89	-	0.5	420.38	4
$La(OH)_3$-doped activated carbon fiber	Room temperature	15.3	10-70	2.5	-	5
Zeolite/$La(OH)_3$	25	71.94	10-500	2.5	55.69	6
Hydrated lanthanum oxide-modified diatomite	25	58.70	10-100	0.5	74.06	7
Flower-like mesoporous silica spheres (FMS-0.2La)	25	44.82	-	0.5	67.4	8
La^{3+}/$La(OH)_3$ loaded magnetic cationic hydrogels (MCH-$La(OH)_3$-EW)	25±1	88.3	0-40	0.3	24.88	9
Lanthanum hydroxide nanorods (LH-3)	-	170.1	0.5-14	0.025	73.8	10

Note: q_m, maximum adsorption capacity; C_0 range, the initial phosphate concentrations to calculate q_m.

Table S4. Adsorption kinetic parameters for phosphate adsorption on MLHO-100C-2.

Kinetic model	Parameter	Initial P concentration	
		5 mg/L	10 mg/L
Experiment value	$q_{e.exp}$ (mg/g)	19.998	39.997
Pseudo-first order	$q_{e.cal}$ (mg/g)	0.464	12.345
	k_1 (1/min)	0.0337	0.0299
	R^2	0.8306	0.9548
Pseudo-second order	$q_{e.cal}$ (mg/g)	20.036	40.519
	k_2 (g/mg min)	0.1058	0.0065
	R^2	0.9999	0.9999

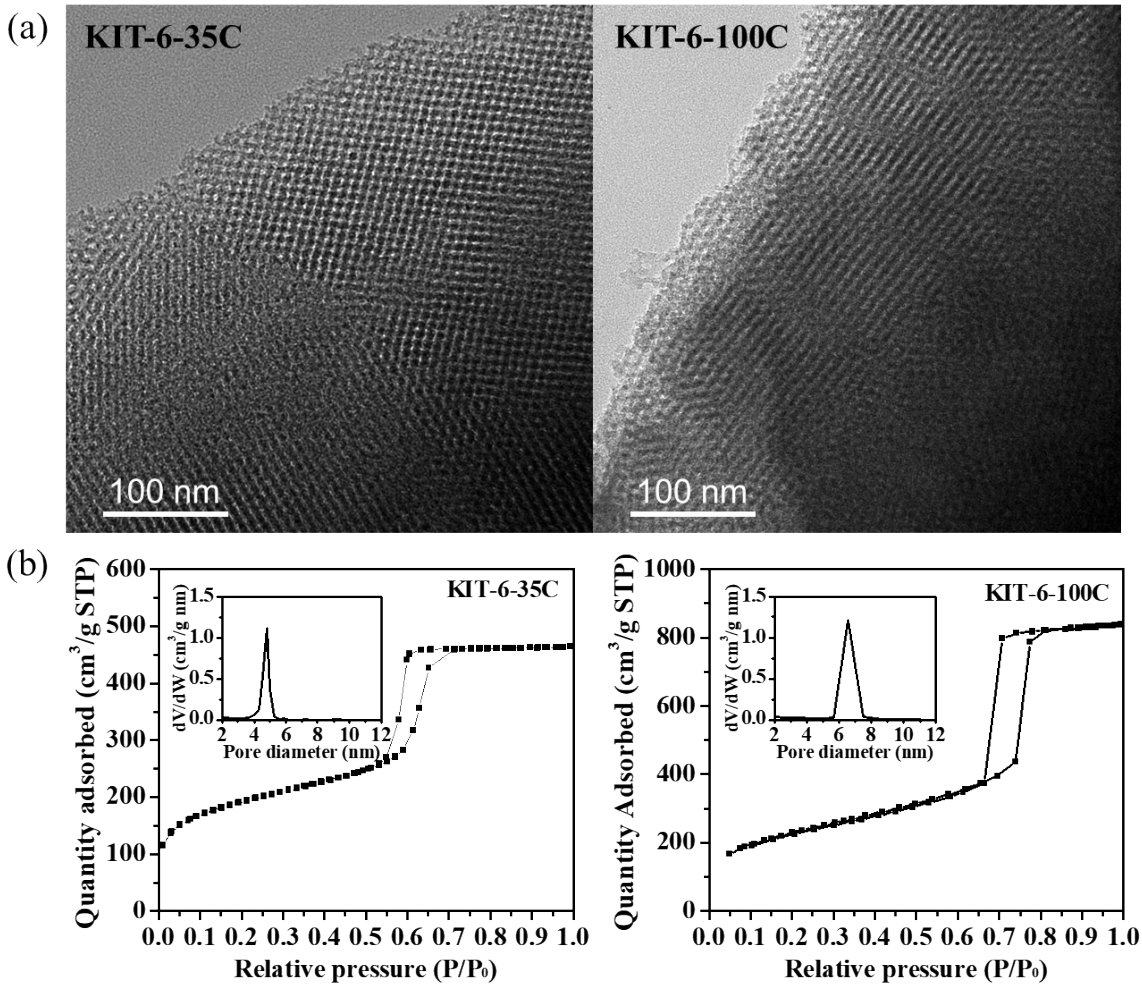

Fig. S1 Characterization of KIT-6 templates. (a) TEM images of KIT-6-35C (left) and KIT-6-100C (right) (b) N_2 adsorption-desorption isotherms and pore size distributions (insets) of KIT-6-35C (left) and KIT-6-100C (right)

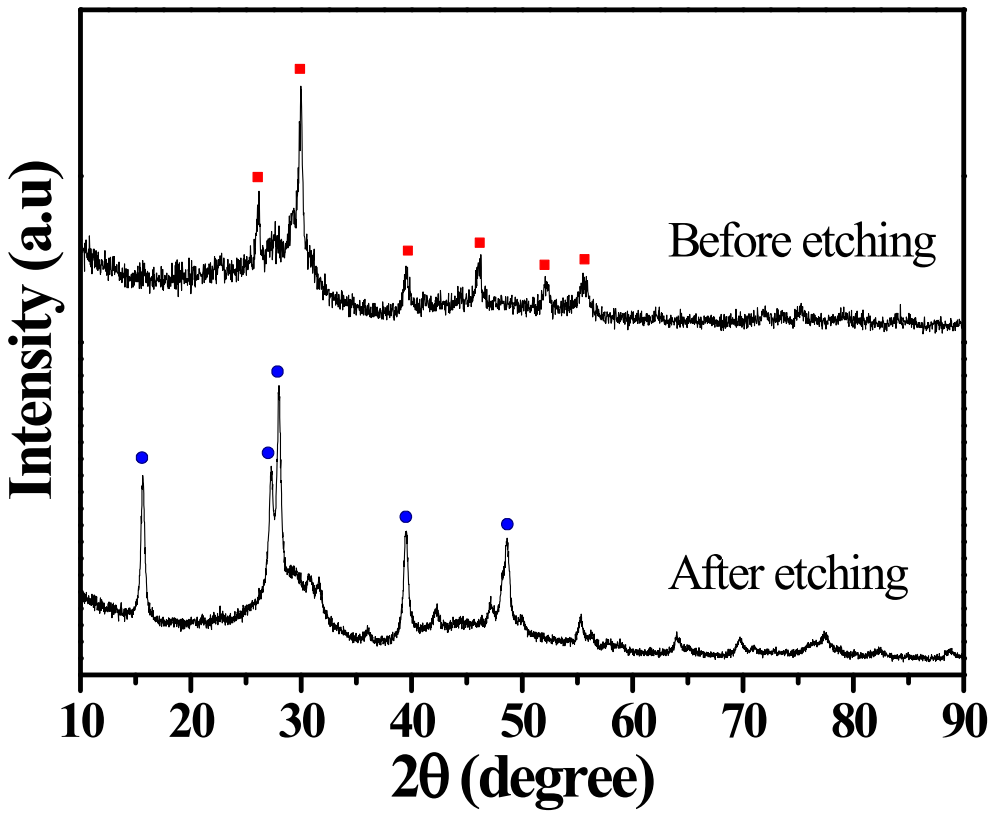

Fig. S2 X-ray diffraction (XRD) patterns of MLHO-35C-4 (bottom) and the composite before etching (top). Red squares and blue circles represent the reference XRD patterns of La_2O_3 (JCPDS#83-1344) and $La(OH)_3$ (JCPDS#31-1481), respectively.

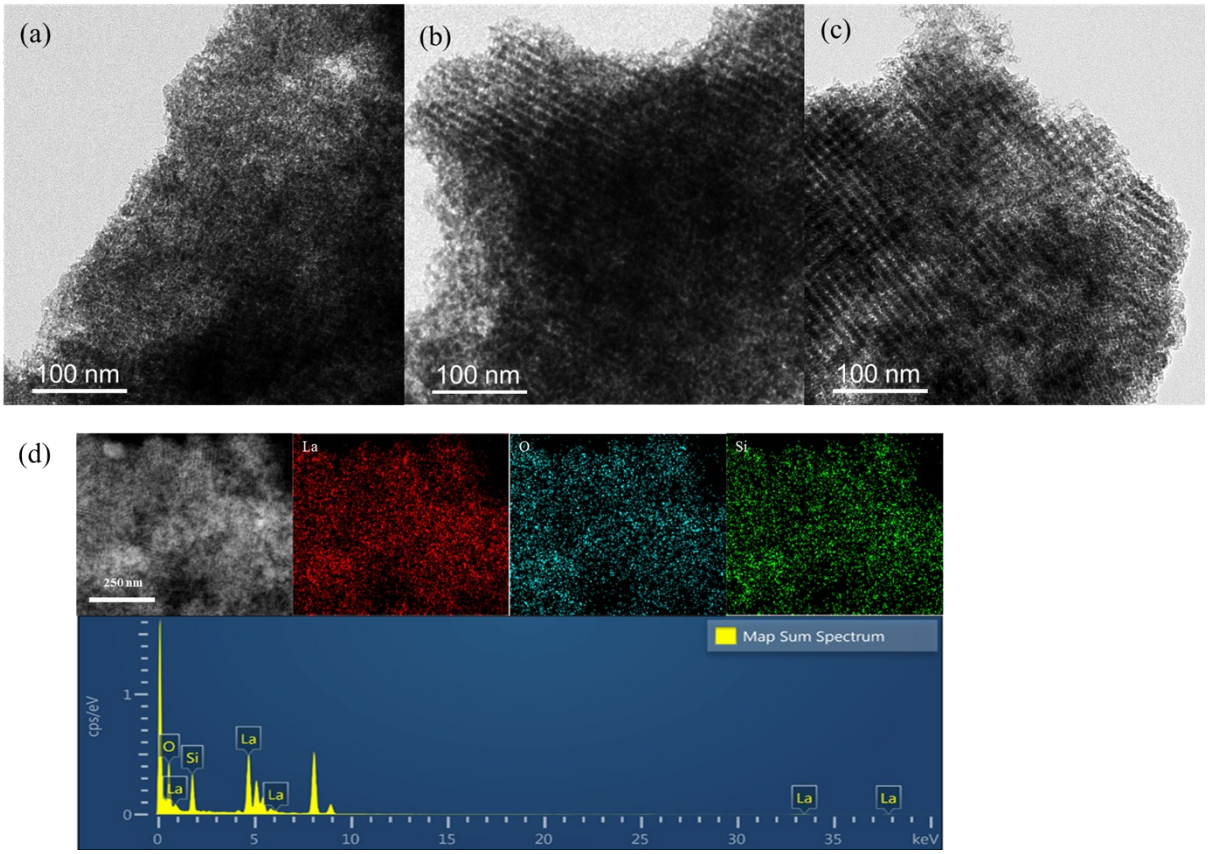

Fig. S3 (a-c) Transmission electron microscopy (TEM) images of MLHO-35Cs: MLHO-35C-2 (a), MLHO-35C-3 (b), and MLHO-35C-4 (c). (d) STEM images with elemental mapping of MLHO-35C-3 after 72 etching

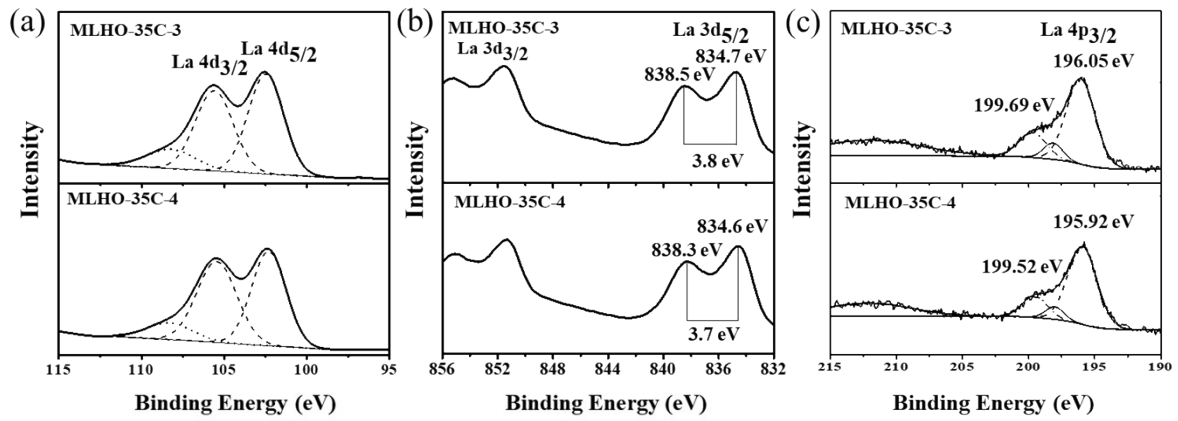

Fig. S4 X-ray photoelectron spectroscopy spectra of MLHO-35Cs: La 4d region (a), La 3d region (b), and La 4p region (c).

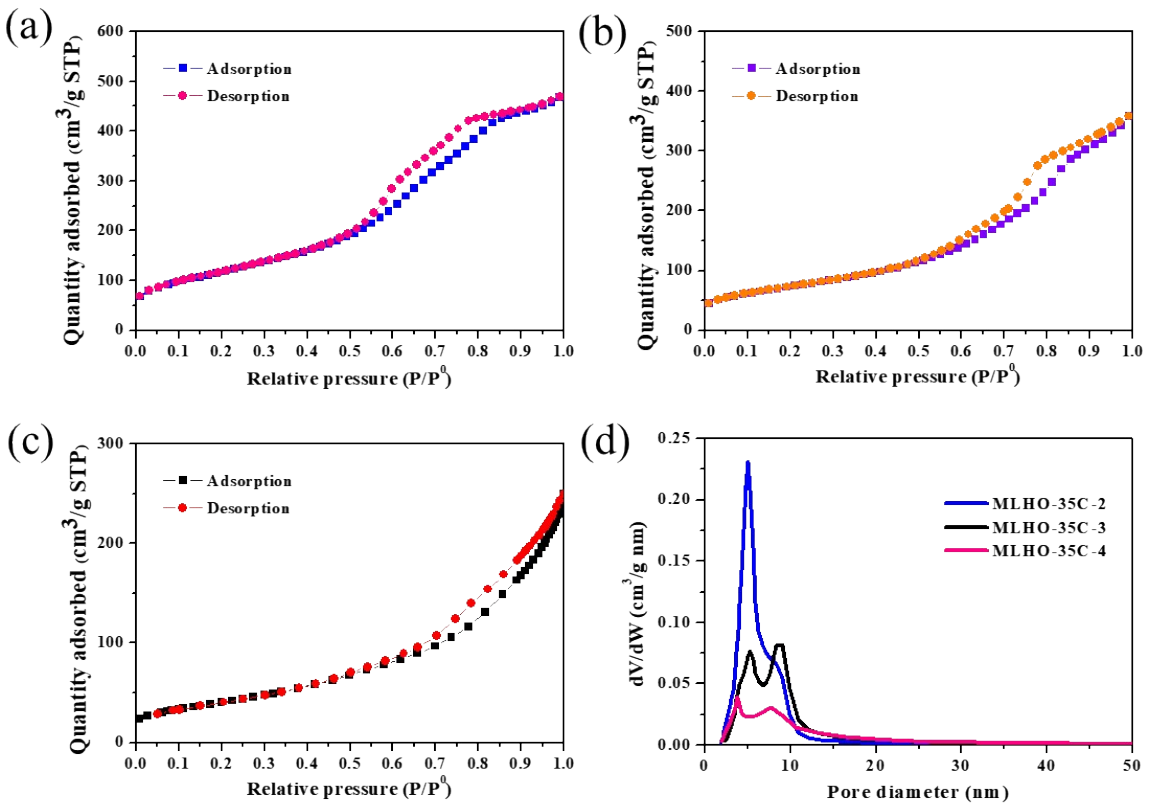

Fig. S5 (a-c) N_2 adsorption/desorption isotherms of MLHO-35C-2 (a), MLHO-35C-3 (b), and MLHO-35C-4 (c). (d) Pore size distributions of MLHO-35Cs calculated by the Barrett-Joiner-Halenda (BJH) method.

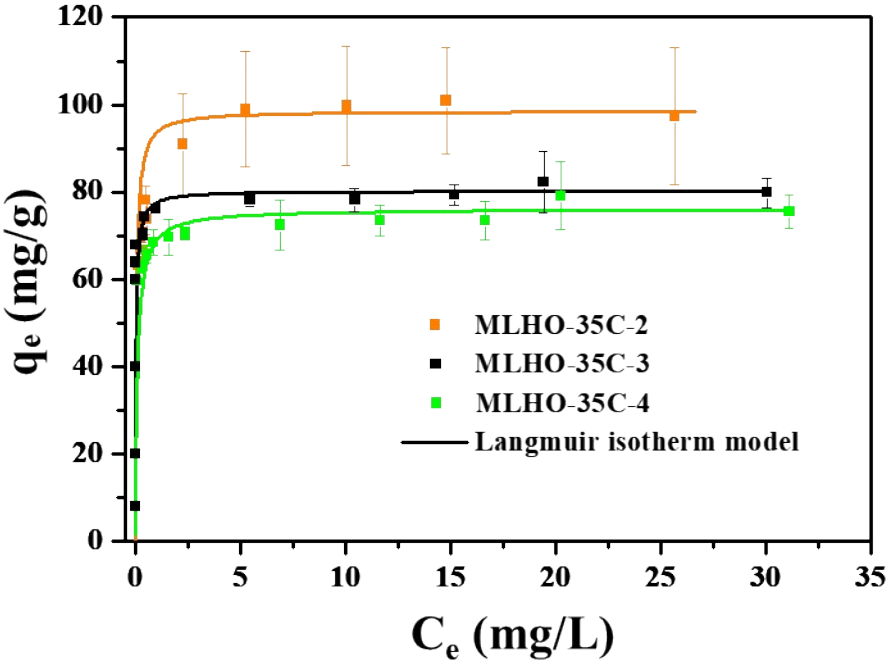

Fig. S6 Adsorption isotherms of phosphate on MLHO-35Cs.

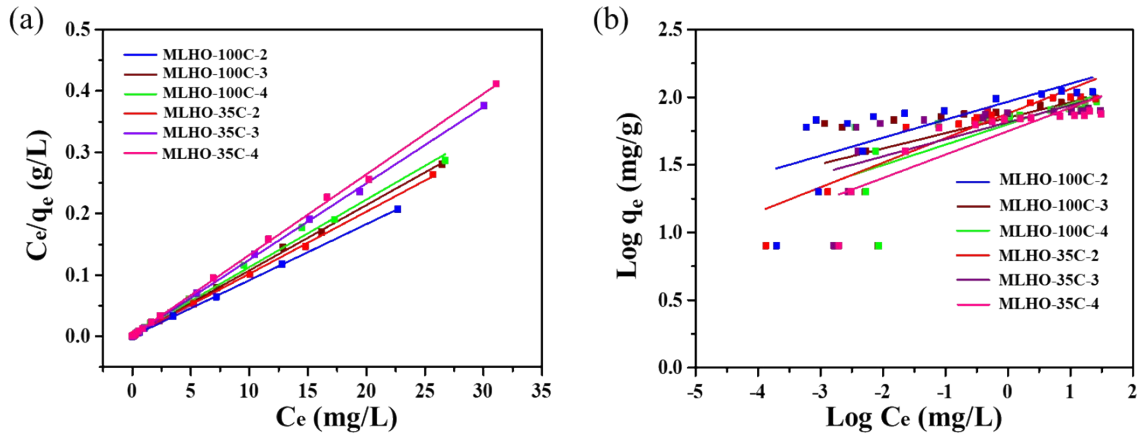

Fig. S7 Langmuir isotherm (a) and Freundlich isotherm (b) fitting plots of the adsorption equilibrium at various phosphate concentrations on MLHOs.

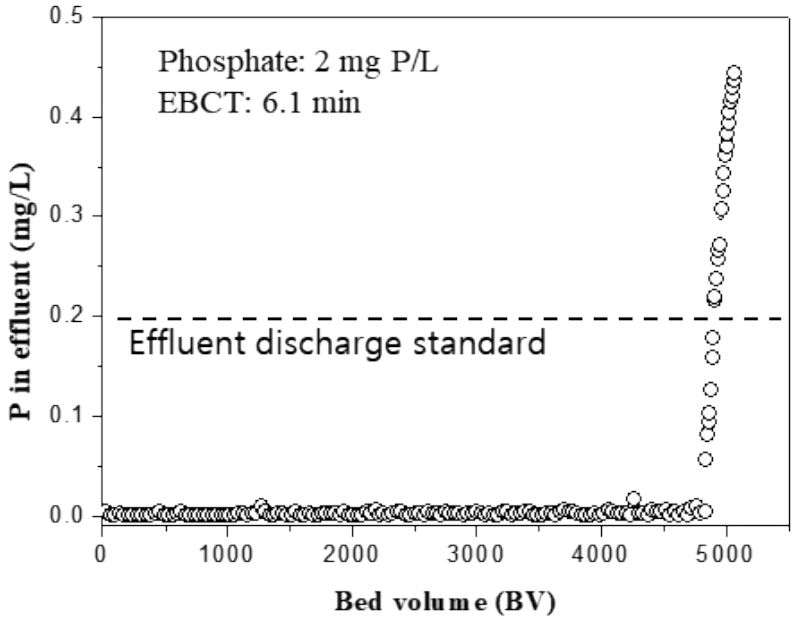

Fig. S8 The breakthrough profile of phosphate removal from feeding solution of 2 mg P/L by MLHO-100C-2. The dashed line represents the effluent discharge standard of WWTPs in Korea (0.2 mg P/L).

References

1 J. Xie, Z. Wang, S. Lu, D. Wu, Z. Zhang and H. Kong, *Chem. Eng. J.*, 2014, **254**, 163-170.

2 J. Xie, Y. Lin, C. Li, D. Wu and H. Kong, *Powder Technol.*, 2015, **269**, 351-357.

3 W.-Y. Huang, D. Li, Z.-Q. Liu, Q. Tao, Y. Zhu, J. Yang and Y.-M. Zhang, *Chem. Eng. J.*, 2014, **236**, 191-201.

4 W. Huang, Y. Zhu, J. Tang, X. Yu, X. Wang, D. Li and Y. Zhang, *J. Mater. Chem. A*, 2014, **2**, 8839-8848.

5 L. Zhang, Q. Zhou, J. Liu, N. Chang, L. Wan and J. Chen, *Chem. Eng. J.*, 2012, **185-186**, 160-167.

6 J. Xie, Z. Wang, D. Fang, C. Li and D. Wu, *J. Colloid Interf. Sci.*, 2014, **423**, 13-19.

7 Y. Wu, X. Li, Q. Yang, D. Wang, Q. Xu, F. Yao, F. Chen, Z. Tao and X. Huang, *J. Environ. Manage.*, 2019, **231**, 370-379.

8 W. Huang, X. Yu, J. Tang, Y. Zhu, Y. Zhang and D. Li, *Microporous Mesoporous Mater.*, 2015, **217**, 225-232.

9 S. Dong, Y. Wang, Y. Zhao, X. Zhou and H. Zheng, *Water Res.*, 2017, **126**, 433-441.

10 L. Fang, B. Wu, J. K. M. Chan and I. M. C. Lo, *Chemosphere*, 2018, **192**, 209-216.